

Reactions of the Cobaltaborane $2,4\text{-}\{\eta^5\text{-C}_5\text{Me}_5\text{Co}\}_2\text{B}_3\text{H}_7$ with Metal Fragments. Synthesis and Characterization of *nido*- $1\text{-}\{\eta^5\text{-C}_5\text{Me}_5\text{Co}\}\text{-}2\text{-}\{(\text{CO})_3\text{Fe}\}\text{B}_3\text{H}_7$ and *arachno*- $(\eta^5\text{-C}_5\text{Me}_5)(\text{CO})\text{CoB}_3\text{H}_7$

Xinjian Lei, Maoyu Shang, and Thomas P. Fehlner*

Department of Chemistry and Biochemistry, University of Notre Dame, Notre Dame, Indiana 46556

Received January 8, 1998

The reactions of *nido*- $2,4\text{-}(\text{Cp}^*\text{Co})_2\text{B}_3\text{H}_7$, **1**, $\text{Cp}^* = (\eta^5\text{-C}_5\text{Me}_5)$, with $\text{Fe}_2(\text{CO})_9$ and $\text{Co}_2(\text{CO})_8$ generate seven skeletal electron pair (sep) *nido*- $1\text{-}\{\text{Cp}^*\text{Co}\}\text{-}2\text{-}\{(\text{CO})_3\text{Fe}\}\text{B}_3\text{H}_7$, **2**, by metal fragment substitution and seven sep *arachno*- $\text{Cp}^*(\text{CO})\text{CoB}_3\text{H}_7$, **3**, by metal fragment degradation. Both compounds are characterized spectroscopically in solution and with single-crystal X-ray diffraction in the solid state. On the basis of the results and related chemistry, the suggested reaction pathway involves $\text{M}(\text{CO})_4$, $\text{M} = \text{Fe}$ and Co , coordination to a $\text{Co}\text{-H}\text{-B}$ edge of **1** followed by loss of $\text{Cp}^*\text{Co}(\text{CO})$ which leads to **2**. We postulate that the cobalt analogue of **2**, which would be an odd-electron species, readily loses a cobalt carbonyl fragment to form **3**.

Introduction

Although the isolobal analogy draws useful connections between many main-group fragments and transition-metal fragments,^{1,2} the properties of a borane fragment make it particularly suitable as a surrogate for a metal fragment in a cluster bonding network.^{3,4} Thus, one of the advantages offered by the study of metallaborane clusters is that the more limited bonding capabilities of the borane fragment can be used to circumscribe the behavior of the metal fragment. This is particularly valuable in the study of cluster reactivity because, isolobal analogy or not, the reaction properties of metal and borane clusters are very different. Thus, variation of the boron-to-metal ratio for a given cluster size and geometry allows the unique properties of the metal centers to be expressed in a systematic fashion.⁵

This aspect of metallaborane chemistry is poorly evidenced in the literature simply because the synthetic chemistry is still in an emerging state.^{6–8} For monometallic compounds there are several systematic methods of value, but for multimetallic compounds there are very few indeed.⁹ Yet when a metallaborane can be made in good yield from easily accessible starting materials, a study of its reactivity reveals a novel and interesting chemistry that parallels, but differs from,

that of related organometallic compounds, e.g., the beautiful development of the reactivity of $\text{H}_3\text{Os}_3(\text{CO})_9\text{-BCO}$ with connections to the isoelectronic $\text{H}_2\text{Os}_3(\text{CO})_9\text{-CCO}$ organometallic compound.^{10–15} Consequently, there is considerable merit in seeking new routes and developing the reaction chemistry of the compounds that result from successful efforts.

We have recently described a potentially general route to dimetallaboranes of the type $\{\text{Cp}^*\text{M}\}_2\text{B}_n\text{H}_{n+4}$ ($\text{Cp}^* = \eta^5\text{-C}_5\text{Me}_5$, $\text{M} = \text{Co}$,¹⁶ Rh ,¹⁷ Cr ,¹⁸ and Mo ,¹⁹ based on the reaction of monocyclopentadienylmetal chloride dimers with monoboranes. Good yields of single products from simple reactions permit the reaction chemistry to be investigated. We have previously reported some of this chemistry for Co ,²⁰ Cr ,²¹ and Mo ²² and in the following describe the reactivity of a *nido*-dicobaltapentaborane with typical metal fragments. Two new metallaboranes are produced in modest to good yield by

- (1) Mingos, D. M. P.; Wales, D. J. *Introduction to Cluster Chemistry*; Prentice Hall: New York, 1990.
- (2) Mingos, D. M. P. In *Inorganometallic Chemistry*; Fehlner, T. P., Ed.; Plenum: New York, 1992; p 179.
- (3) Fehlner, T. P. *Adv. Inorg. Chem.* **1990**, *35*, 199.
- (4) Fehlner, T. P. *Structure and Bonding* **1997**, *87*, 112.
- (5) Fehlner, T. P. In *Electron Deficient Boron and Carbon Clusters*; Olah, G. A., Wade, K., Williams, R. E., Eds.; Wiley: New York, 1991; p 287.
- (6) Kennedy, J. D. *Prog. Inorg. Chem.* **1984**, *32*, 519.
- (7) Kennedy, J. D. *Prog. Inorg. Chem.* **1986**, *34*, 211.
- (8) Grimes, R. N. In *Metal Interactions with Boron Clusters*; Grimes, R. N., Ed.; Plenum: New York, 1982; p 269.
- (9) Housecroft, C. E. In *Inorganometallic Chemistry*; Fehlner, T. P., Ed.; Plenum Press: New York, 1992; p 33.

- (10) Chung, J.-H.; Boyd, E. P.; Liu, J.; Shore, S. G. *Inorg. Chem.* **1997**, *36*, 4778.
- (11) DeKock, R. L.; Deshmukh, P.; Fehlner, T. P.; Housecroft, C. E.; Plotkin, J. S.; Shore, S. G. *J. Am. Chem. Soc.* **1983**, *105*, 815.
- (12) Jan, D.-Y.; Hsu, L.-Y.; Workman, D. P.; Shore, S. G. *Organometallics* **1987**, *6*, 1984.
- (13) Jan, D.-Y.; Shore, S. G. *Organometallics* **1987**, *6*, 428.
- (14) Jan, D.-Y.; Workman, D. P.; Hsu, L.-Y.; Krause, J. A.; Shore, S. G. *Inorg. Chem.* **1992**, *31*, 5123.
- (15) Workman, D. P.; Deng, H. B.; Shore, S. G. *Angew. Chem., Int. Ed. Engl.* **1990**, *29*, 309–311.
- (16) Nishihara, Y.; Deck, K. J.; Shang, M.; Fehlner, T. P.; Haggerty, B. S.; Rheingold, A. L. *Organometallics* **1994**, *13*, 4510.
- (17) Lei, X.; Shang, M.; Fehlner, T. P. *J. Am. Chem. Soc.* **1998**, *120*, 2686.
- (18) Ho, J.; Deck, K. J.; Nishihara, Y.; Shang, M.; Fehlner, T. P. *J. Am. Chem. Soc.* **1995**, *117*, 10292.
- (19) Aldridge, S.; Fehlner, T. P.; Shang, M. *J. Am. Chem. Soc.* **1997**, *119*, 2339.
- (20) Deck, K. J.; Brenton, P.; Fehlner, T. P. *Inorg. Chem.* **1997**, *36*, 554.
- (21) Hashimoto, H.; Shang, M.; Fehlner, T. P. *Organometallics* **1996**, *15*, 1963.
- (22) Aldridge, S.; Hashimoto, H.; Kawamura, K.; Shang, M.; Fehlner, T. P. *Inorg. Chem.* **1998**, *37*, 928.

metal fragment substitution in one case and metal fragment loss in the other. The former has been observed in related organometallic clusters²³ as well as metallaborane chemistry.²⁴ The latter constitutes a new route to so-called "borallyl" complexes previously prepared from $[B_3H_8]^-$ and mononuclear metal complexes of Ir,^{25,26} Pd,^{27,28} and Pt^{29–31} with phosphine ancillary ligands. Here a first-row transition-metal analogue is synthesized by building up a B_3H_7 fragment on a dicobalt framework followed by removal of one metal fragment. A previous attempt to make a cobalt borallyl complex by reacting $(PPh_3)_2CoCl_2$ with $[B_3H_8]^-$ led only to the phosphine adduct $B_3H_7PPh_3$.²⁵

Experimental Section

General. All operations were conducted under a dinitrogen atmosphere using standard Schlenk techniques.³² Solvents were distilled before use under N_2 as follows: sodium benzophenone ketyl for hexane, diethyl ether, and tetrahydrofuran. The starting material *nido*-2,4-(Cp*Co)₂B₃H₇, **1**, was prepared according to published procedures.¹⁶ Fe₂(CO)₉ (Aldrich) and Co₂(CO)₈ (Strem) were used as received. NMR spectra were recorded on a 300 or 500 MHz Varian FT-NMR spectrometer. The solvent proton signal was used as a reference for ¹H NMR (δ , ppm, benzene, 7.15), while a sealed tube containing $[Et_4N][B_3H_8]$ in acetone-*d*₆ (−29.7 ppm) was used as the external reference for ¹¹B NMR. Infrared spectra were obtained on a Nicolet 205 FT-IR spectrometer. Mass spectra were obtained on a Finnigan MAT model 8400 mass spectrometer with EI mode. Perfluorokerosene was used as the standard for the high-resolution EI mass spectra. Elemental analysis was performed by M-H-W Laboratories, Phoenix, AZ.

***nido*-1-(Cp*Co)-2-[(CO)₃Fe]B₃H₇, **2**.** In a 200 mL Schlenk tube, *nido*-2,4-(Cp*Co)₂B₃H₇, **1** (0.40 g, 0.94 mmol), and Fe₂(CO)₉ (0.43 g, 1.18 mmol) were loaded. A 15 mL amount of freshly distilled toluene was slowly added to the mixture by syringe. The reaction mixture was stirred at ca. 50 °C for 6 h. During this period, a black solid and a dark brown solution were observed to form. The toluene was then removed under vacuum, and the resulting residue was extracted with hexane and filtered through Celite. Low-temperature column chromatography (−40 °C) was performed. Elution with hexane gave a brown solution of **2** in 28% (0.10 g) yield. Elution with 3% ether in hexane afforded 0.47 g of a dark brown solid which contained Cp*Co(CO)₂ (FAB, P⁺ = 250 and IR (hexane, cm^{−1}) 2010 s, 1949 s) and unknown carbonyl compounds (IR (hexane, cm^{−1}) 2037 w, 2022 m, 1975 m, 1957 m).

Spectroscopic data for **2**: MS (EI), P⁺ = 374, 3 boron atoms, fragment peaks corresponding to sequential loss of three CO. Calcd for ¹²C₁₃¹H₂₂¹⁶O₃¹¹B₃⁵⁹Co⁵⁷Fe, 374.0529; obsd, 374.0551. NMR: ¹¹B (hexane, 22 °C) δ 13.7 (d, J_{B-H} = 146 Hz, {¹H}, s,

1B), 1.4 (d, J_{B-H} = 146 Hz, {¹H}, s, 2B); ¹H (C₆D₆, 22 °C) δ 3.7 (q, 1H, BH_t, J_{B-H} = 148 Hz), 3.1 (q, 2H, BH_t, J_{B-H} = 143), 1.7 (s, 15H, C₅Me₅), −3.8 (s, 2H, B–H–B), −14.7 (d, 2H, Fe–H–B). IR (hexane, cm^{−1}): 2525 w, 2489 w (B–H); 2056 s, 2000 s (CO). Anal. Calcd for C₁₃H₂₂O₃B₃CoFe: C, 41.80; H, 5.94. Found: C, 41.67; H, 6.07.

***arachno*-Cp*(CO)CoB₃H₇, **3**.** In a 100 mL Schlenk tube, **1** (0.21 g, 0.51 mmol) and Co₂(CO)₈ (0.21 g, 0.51 mmol) were loaded. The mixture was chilled to −40 °C, and 10 mL of freshly distilled toluene was added slowly by plastic syringe. The reaction mixture was allowed to warm gradually up room temperature and stirred for 20 h. During this period, a black solid and a dark brown solution were observed to form. The toluene was then removed under vacuum, and the resulting residue was extracted with hexane and filtered through Celite. The solution was kept at −40 °C. Black needlelike crystals which were identified as Co₄(CO)₁₂ were removed by filtration. The filtrate was concentrated and kept at −40 °C. The fractional crystallization procedure was repeated several times until the solution IR showed very weak carbonyl bands due to Co₄(CO)₁₂. Then low-temperature column chromatography (−40 °C) was performed (elution with 3% ether in hexane). A dark brown solution was collected. Recrystallization gives 54 mg of air-sensitive brown crystals of **3** with a yield of 41%. The IR of the remaining solution indicated Cp*Co(CO)₂ (2009, 1948 cm^{−1}) to be another major coproduct.

Spectroscopic data for **3**: MS (EI), P⁺ = 262, 3 boron atoms; fragment peak at 234 corresponding to loss of one CO. Calcd for ¹²C₁₁¹H₂₂¹⁶O¹¹B₃⁵⁹Co, 262.1288; obsd, 262.1294. NMR: ¹¹B (hexane, 22 °C) δ 6.1 (doublet–triplet, J_{B-H} = 140, 40 Hz, {¹H}, s, 1B), −0.8 (t, J_{B-H} = 126 Hz, {¹H}, s, 2B); ¹H (C₆D₆, 22 °C) δ 3.1 (overlapping quartet, 4H, BH_t), 2.9 (overlapping quartet, 1H, BH_t), 1.4 (s, 15H, C₅Me₅), −4.0 (s, 2H, B–H–B). IR (hexane, cm^{−1}): 2532 w, 2498 w, 2441 w (B–H); 2018 s (CO).

X-ray Structure Determinations. *nido*-1-(Cp*Co)-2-[(CO)₃Fe]B₃H₇, **2.** After column chromatography, the brown hexane solution was saturated by removing the solvent in vacuo. After 10 days in a freezer at −40 °C, large black crystals suitable for diffraction were obtained. Diffraction data were collected at a temperature of 20 °C with an Enraf-Nonius CAD4 diffractometer equipped with a graphite-monochromatic Mo K α X-radiation source using the $\omega/2\theta$ scan technique. SDP software was used to process the intensity data.³³ Lorentz and polarization corrections and a linear decay correction were applied to the data. An empirical absorption correction based on ψ scans was also applied to the data. Structure solution and refinement were performed on a PC by using the SHELXL-TL package.³⁴ Most of the non-hydrogen atoms were located by the direct method; the remaining non-hydrogen atoms were found in succeeding difference Fourier synthesis. Least-squares refinement was carried out on F^2 for all reflections. After all non-hydrogen atoms were refined anisotropically, difference Fourier synthesis located all hydrogen atoms. In the final refinement, methyl hydrogen atoms were refined with a riding model while the borane hydrogens were refined isotropically with bond length restraints. The refinement converged to final values of R_1 = 0.0229 and wR_2 = 0.0625 for observed unique reflections ($I > 2\sigma(I)$) and R_1 = 0.0258 and wR_2 = 0.0651 for all unique reflections, including those with negative intensities. Detailed crystallographic data are given in Table 1.

***arachno*-Cp*(CO)CoB₃H₇, **3**.** After column chromatography, the dark-brown hexane solution was saturated by removing the solvent in vacuo. After 3 days inside a freezer at −40 °C, large polyhedral brown crystals along with black needles

(23) *The Chemistry of Metal Cluster Complexes*; Shriver, D. F., Kaesz, H. D., Adams, R. D., Eds.; VCH: New York, 1990.

(24) Jun, C.-S.; Bandyopadhyay, A. K.; Fehlner, T. P. *Inorg. Chem.* **1996**, *35*, 2189.

(25) Greenwood, N. N.; Kennedy, J. D.; Reed, D. *J. Chem. Soc., Dalton Trans.* **1980**, 196.

(26) Bould, J.; Greenwood, N. N.; Kennedy, J. D.; McDonald, W. S. *J. Chem. Soc., Dalton Trans.* **1985**, 1843.

(27) Housecroft, C. E.; Shaykh, B. A. M.; Rheingold, A. L.; Haggerty, B. S. *Inorg. Chem.* **1991**, *30*, 125.

(28) Housecroft, C. E.; Owen, S. M.; Raithby, P. R.; Shaykh, B. A. M. *Organometallics* **1990**, *9*, 1617.

(29) Bould, J.; Kennedy, J. D.; McDonald, W. S. *Inorg. Chim. Acta* **1992**, *196*, 201.

(30) Guggenberger, L. J.; Kane, A. R.; Muetterties, E. L. *J. Am. Chem. Soc.* **1972**, *94*, 5665.

(31) Haggerty, B. S.; Housecroft, C. E.; Rheingold, A. L.; Shaykh, B. A. M. *J. Chem. Soc., Dalton Trans.* **1991**, 2175.

(32) Shriver, D. F.; Drezdson, M. A. *The Manipulation of Air-Sensitive Compounds*, 2nd ed.; Wiley-Interscience: New York, 1986.

(33) Frenz, B. A. In *The Enraf-Nonius CAD4—A Real-time System for Concurrent X-ray Data Collection and Crystal Structure Determination*; Schenk, H., Olthof-Hazelkamp, R., von Konigsveld, H., Bassi, G. C., Eds.; Delft University Press: Delft, Holland, 1978; p 64.

(34) Sheldrick, G. M. Siemens Industrial Automation Inc.: Madison, WI, 1994.

Table 1. Crystal Data and Structure Refinement for *nido*-1- $\{(\eta^5\text{-C}_5\text{Me}_5)\text{Co}\}$ -2- $\{\text{Fe}(\text{CO})_3\}\text{B}_3\text{H}_7$, **2**, and *arachno*-($\eta^5\text{-C}_5\text{Me}_5$)(CO)CoB₃H₇, **3**

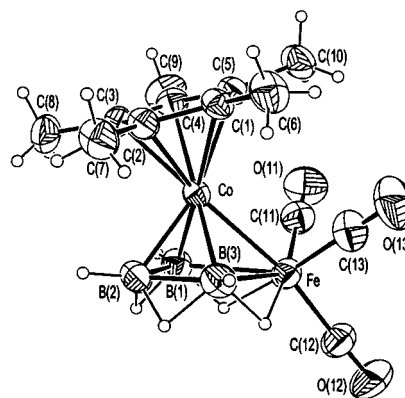
	2	3
fw	373.52	261.65
cryst syst	monoclinic	monoclinic
space group	<i>C2/c</i>	<i>P2₁/n</i>
<i>a</i> (Å)	29.204(3)	7.0216(11)
<i>b</i> (Å)	8.5268(6)	27.298(2)
<i>c</i> (Å)	15.905(3)	8.0282(12)
β , deg	120.803(13)	111.739(6)
volume (Å ³)	3401.9(8)	1429.4(3)
<i>Z</i>	8	4
<i>D_c</i> (Mg/m ³)	1.459	1.216
<i>F</i> (000)	1536	552
wavelength (Å)	0.710 73	0.710 73
abs coeff (mm ⁻¹)	1.830	1.176
cryst size (mm)	0.38 × 0.28 × 0.15	0.38 × 0.35 × 0.30
temp (K)	293(2)	293(2)
diffractometer	Enraf-Nonius CAD4	Enraf-Nonius CAD4
θ range, deg	2.52–24.98	2.83–25.00
total no. of data collected	5949	2712
no. of unique data	2974	2510
	[<i>R</i> (int) = 0.0140]	[<i>R</i> (int) = 0.0142]
no. of unique obsd data [<i>I</i> > 2 σ (<i>I</i>)]	2750	2240
abs corr	ψ scans	ψ scans
max and min transmission	0.9994 and 0.8160	0.9983 and 0.8563
refinement method	SHELXL-93	SHELXL-93
weighting scheme	σ weight	σ weight
data/restraints/params	2974/0/279	2485/9/175
goodness-of-fit on <i>F</i> ²	1.090	1.157
final <i>R</i> indices [<i>I</i> > 2 σ (<i>I</i>)]	<i>R</i> ₁ ^a = 0.0229	<i>R</i> ₁ ^a = 0.0470
<i>R</i> indices (all data)	<i>wR</i> ₂ ^b = 0.0625 <i>R</i> ₁ ^a = 0.0258 <i>wR</i> ₂ ^b = 0.0651	<i>wR</i> ₂ ^b = 0.1168 <i>R</i> ₁ ^a = 0.0552 <i>wR</i> ₂ ^b = 0.1505

$$^a R = \sum ||F_o| - |F_c|| / \sum |F_o|. \quad ^b wR = [\sum w(F_o^2 - F_c^2)^2 / \sum w(F_o^2)^2]^{1/2}.$$

of Co₄(CO)₁₂ (IR) were found. Diffraction data on a polyhedral crystal were collected at a temperature of 20 °C with an Enraf-Nonius CAD4 diffractometer equipped with a graphite-monochromatic Mo K α X-radiation source using the $\omega/2\theta$ scan technique. SDP software was used to process the intensity data. Lorentz and polarization corrections and a linear decay correction were applied to the data. An empirical absorption correction based on ψ scans was also applied to the data. Structure solution and refinement were performed on a PC by using the SHELXTL package. Most of the non-hydrogen atoms were located by the direct method; the remaining non-hydrogen atoms were found in succeeding difference Fourier synthesis. Least-squares refinement was carried out on *F*² for all reflections. After all non-hydrogen atoms were refined anisotropically, difference Fourier synthesis located all hydrogen atoms. In the final refinement, methyl hydrogen atoms were refined with a riding model while the borane hydrogens were refined isotropically with bond length restraints. The refinement converged to final values of *R*₁ = 0.0470 and *wR*₂ = 0.1168 for observed unique reflections (*I* > 2 σ (*I*)) and *R*₁ = 0.0552 and *wR*₂ = 0.1505 for all unique reflections, including those with negative intensities. Detailed crystallographic data are given in Table 1.

Results and Discussion

Structures. The reactions of 2,4-(Cp*Co)₂B₃H₇, **1**, with Fe₂(CO)₉ and Co₂(CO)₈ generate two new metallaboranes. The identities of these two compounds are clearly indicated by the spectroscopic data. For **2**, the data suggest a dimetal derivative of the seven skeletal electron pair (sep) *nido*-B₃H₉, and for **3**, the data suggest a monometal derivative of the seven sep *arachno*-B₄H₈-CO. The spectral interpretations constitute nice ex-

**Figure 1.** Molecular structure of *nido*-1-(Cp*Co)-2- $\{(\text{CO})_3\text{Fe}\}\text{B}_3\text{H}_7$, **2**, with thermal ellipsoids at 40% probability.

amples of the application of the electron counting rules as both Cp*Co and Fe(CO)₃ fragments are isolobal with BH.^{35,36} Of course, in the case of **2**, the spectroscopic data do not allow the two possible isomers 1-(Cp*Co)-2- $\{(\text{CO})_3\text{Fe}\}\text{B}_3\text{H}_7$ and 1- $\{(\text{CO})_3\text{Fe}\}$ -2-(Cp*Co)B₃H₇ to be distinguished; however, the crystallographic characterization is definitive.

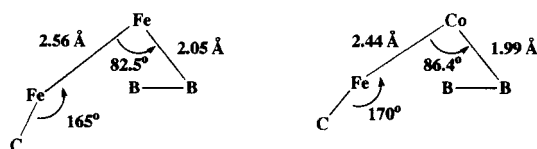
***nido*-1-(Cp*Co)-2- $\{(\text{CO})_3\text{Fe}\}\text{B}_3\text{H}_7$, **2**.** The molecular structure of **2** is shown in Figure 1, and selected distances and angles are given in Table 2. All of the distances and angles fall within the ranges of existing structural data on boranes³⁷ and metallaboranes.³⁸ Clearly, the structure of **2** is derived from that of B₅H₉ in which an apical BH fragment is replaced by Cp*Co and a basal BH fragment by Fe(CO)₃. The compound is most closely related to 1,2- $\{\text{Fe}(\text{CO})_3\}_2\text{B}_3\text{H}_7$ (**2'**)³⁹ and *nido*-1,2-(Cp*Co)(μ -H) $\{(\eta^5\text{-C}_5\text{Me}_5\text{H})\text{Co}\}_2\text{B}_3\text{H}_7$ (**2''**)⁴⁰ but is also a metal fragment positional isomer of 2,4-(Cp*Co)₂B₃H₇⁴⁰ and 2-(Cp*Os)-3- $\{(\text{PPh}_3)_2(\text{CO})\text{Rh}\}\text{B}_3\text{H}_7$.⁴¹

Although **2**, **2'**, and **2''** have the same core structure, there are some significant differences in the structural metrics. Selected comparisons are given in Table 3. For instance, the major differences between **2** and **2'** can be appreciated by looking at the atoms in the M–M–B(2) plane as shown in Chart 1 (B(1) and B(3) are superimposed and do not lie in the plane of the paper). In going from **2'** to **2**, the metal–metal and apical metal–boron distances shorten and the M–M–B and C–M–M angles open. The net result is that the Fe atom, which is distinctly beneath the plane defined by the three boron atoms in **2'** (0.23 Å), lies 0.15 Å above the plane in **2**. The C₃ axis of the basal Fe(CO)₃, which points at B(2) in **2'**, tilts such that it continues to point at B(2) in **2**. The tilt of the plane of the three carbonyl carbon atoms of the apical Fe(CO)₃ of **2'** relative to the B₃ plane is 2.5°, whereas the tilt of the plane of the five carbon atoms of the apical Cp*Co fragment in **2** relative to the B₃ plane is 8.9°. This suggests a greater repulsive

(35) Wade, K. *Adv. Inorg. Chem. Radiochem.* **1976**, *18*, 1.(36) Mingos, D. M. P. *Acc. Chem. Res.* **1984**, *17*, 311–319.(37) Shore, S. G. In *Boron Hydride Chemistry*; Muettterties, E. L., Ed.; Academic Press: New York, 1975; p 79.(38) Housecroft, C. E. *Adv. Organomet. Chem.* **1991**, *33*, 1.(39) Andersen, E. L.; Haller, K. J.; Fehlner, T. P. *J. Am. Chem. Soc.* **1979**, *101*, 4390.(40) Nishihara, Y.; Deck, K. J.; Shang, M.; Fehlner, T. P. *J. Am. Chem. Soc.* **1993**, *115*, 12224.(41) Bould, J.; Pasieka, M.; Braddock-Wilking, J.; Rath, N. P.; Barton, L.; Gloeckner, C. *Organometallics* **1995**, *14*, 5138.

Table 2. Selected Bond Lengths (Å) and Angles (deg) for *nido-1-[(η⁵-C₅Me₅)Co]-2-[(CO)₃Fe]B₃H₇, 2*

Co-Fe	2.4443(4)	Fe-H(1)	1.66(3)
Co-B(2)	1.975(2)	Fe-H(6)	1.67(3)
Co-B(3)	1.999(3)	B(1)-B(2)	1.785(4)
Co-B(1)	2.005(2)	B(2)-B(3)	1.778(4)
Co-C(2)	2.054(2)	B(1)-H(1)	1.29(2)
Co-C(3)	2.054(2)	B(1)-H(2)	1.28(3)
Co-C(1)	2.092(2)	B(1)-H(3)	1.01(2)
Co-C(4)	2.093(2)	B(2)-H(2)	1.21(3)
Co-C(5)	2.115(2)	B(2)-H(4)	1.24(3)
Fe-C(11)	1.770(3)	B(2)-H(5)	1.05(3)
Fe-C(13)	1.776(3)	B(3)-H(4)	1.32(3)
Fe-C(12)	1.800(3)	B(3)-H(6)	1.29(3)
Fe-B(3)	2.243(3)	B(3)-H(7)	1.07(3)
Fe-B(1)	2.248(3)		
B(2)-Co-B(3)	53.13(11)	H(1)-B(1)-H(3)	105(2)
B(2)-Co-B(1)	53.27(11)	H(2)-B(1)-H(3)	107(2)
B(3)-Co-B(1)	81.07(11)	B(3)-B(2)-B(1)	93.9(2)
B(2)-Co-Fe	86.36(8)	B(3)-B(2)-Co	64.12(11)
B(3)-Co-Fe	59.64(8)	B(1)-B(2)-Co	64.20(11)
B(1)-Co-Fe	59.72(7)	B(3)-B(2)-H(2)	114.5(14)
B(3)-Fe-B(1)	70.83(10)	B(1)-B(2)-H(2)	45.9(13)
B(3)-Fe-Co	50.27(7)	Co-B(2)-H(2)	110.1(14)
B(1)-Fe-Co	50.37(6)	B(3)-B(2)-H(4)	48.0(13)
B(3)-Fe-H(1)	89.0(8)	B(1)-B(2)-H(4)	112.2(13)
B(1)-Fe-H(1)	34.7(8)	Co-B(2)-H(4)	112.0(14)
Co-Fe-H(1)	84.8(9)	H(2)-B(2)-H(4)	95(2)
B(3)-Fe-H(6)	34.8(9)	B(3)-B(2)-H(5)	133.2(13)
B(1)-Fe-H(6)	90.2(9)	B(1)-B(2)-H(5)	131.8(13)
Co-Fe-H(6)	85.0(9)	Co-B(2)-H(5)	121.2(13)
H(1)-Fe-H(6)	89.2(12)	H(2)-B(2)-H(5)	107(2)
O(11)-C(11)-Fe	177.4(2)	H(4)-B(2)-H(5)	108(2)
O(12)-C(12)-Fe	177.5(3)	B(2)-B(3)-Co	62.74(11)
O(13)-C(13)-Fe	178.7(3)	B(2)-B(3)-Fe	97.72(14)
B(2)-B(1)-Co	62.53(11)	Co-B(3)-Fe	70.09(8)
B(2)-B(1)-Fe	97.36(14)	B(2)-B(3)-H(4)	44.4(12)
Co-B(1)-Fe	69.91(7)	Co-B(3)-H(4)	107.0(10)
B(2)-B(1)-H(1)	112.9(11)	Fe-B(3)-H(4)	111.3(12)
Co-B(1)-H(1)	116.4(11)	B(2)-B(3)-H(6)	114.9(11)
Fe-B(1)-H(1)	47.0(11)	Co-B(3)-H(6)	117.3(12)
B(2)-B(1)-H(2)	42.6(13)	Fe-B(3)-H(6)	47.4(12)
Co-B(1)-H(2)	105.1(13)	H(4)-B(3)-H(6)	93(2)
Fe-B(1)-H(2)	113.4(13)	B(2)-B(3)-H(7)	128(2)
H(1)-B(1)-H(2)	95(2)	Co-B(3)-H(7)	122(2)
B(2)-B(1)-H(3)	131.3(14)	Fe-B(3)-H(7)	134(2)
Co-B(1)-H(3)	124.1(13)	H(4)-B(3)-H(7)	107(2)
Fe-B(1)-H(3)	131.1(14)	H(6)-B(3)-H(7)	106(2)

Chart 1

interaction between the metal fragment ligands in **2** than in **2'**, but the metal-metal distance is still shorter in the former.

These quantitative differences in the structures of **2** and **2'** are due to the fact that although Cp*Co and Fe(CO)₃ are isolobal, they perturb a bonding partner in different ways. In fact, the shorter metal-metal and metal-boron distances in going from **2'** to **2** are fully consistent with an earlier analysis of the differences between the bonding capabilities of the M(CO)₃ and M(CH)_n fragments.⁴² That is, a CpM fragment leads to shorter M-M and M-E (E = main-group atom) bonds due to a stronger σ-bonding effect and an oxidation-state effect, respectively.

(42) Elian, M.; Chen, M. M. L.; Mingos, D. M. P.; Hoffmann, R. *Inorg. Chem.* **1976**, *15*, 1148.

Table 3. Comparison of Structural Parameters of the *nido-1,2*-Bimetallopentaboranes *nido-1-[(η⁵-C₅Me₅)Co]-2-[(CO)₃Fe]B₃H₇, 2, *nido-1,2-[(η⁵-C₅Me₅)Co]-2-[(CO)₃Fe]B₃H₇, 2', and *nido-1,2-[(η⁵-C₅Me₅)Co](μ-H){(C₅Me₅H)Co}B₃H₇, 2''***

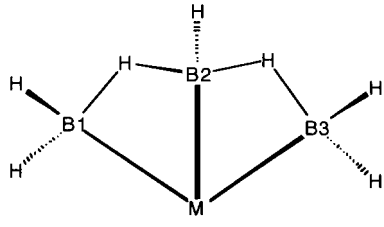
	2 ^a	2' ^b	2'' ^c
Distances, Å			
M1-M2	2.4443(4)	2.559(2)	2.5260(5)
M1-B1	2.005(2)	2.070(4)	2.035(4)
M1-B2	1.975(2)	2.054(5)	1.984(4)
M1-B3	1.999(3)	2.065(4)	2.035(3)
M2-B1	2.248(3)	2.275(4)	2.230(4)
M2-B3	2.243(3)	2.251(4)	2.219(3)
B1-B2	1.785(4)	1.774(6)	1.810(6)
B2-B3	1.778(4)	1.780(6)	1.801(6)
Angles, Deg			
B1-M1-B3	81.0(1)	77.69(18)	80.7(2)
B1-M1-B2	53.27(11)	50.96(18)	53.5(2)
B2-M1-B3	53.13(11)	51.21(19)	53.2(2)
B1-B2-B3	93.9(2)	93.7(20)	93.7(2)
B1-M2-B3	70.83(10)	69.92(16)	72.6(1)
B1-M1-M2	59.72(7)	57.71(12)	57.2(2)
B2-M1-M2	86.36(8)	82.46(15)	83.1(1)
M2-H _b -B	98.0(3)	101(5)	102(4)
B-H _b -B	89(2)	87(2)	88.4(6)

^a This work, M1 = Co, M2 = Fe. ^b Reference 39, M1 = M2 = Fe. ^c Reference 40, M1 = M2 = Co.

Table 4. Selected Bond Lengths (Å) and Angles (deg) for *arachno-(η⁵-C₅Me₅)(CO)CoB₃H₇, 3*

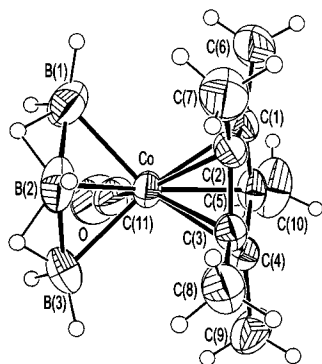
Co-B(1)	2.098(6)	B(1)-B(2)	1.853(11)
Co-B(2)	2.014(6)	B(1)-H(1)	1.09(2)
Co-B(3)	2.096(6)	B(1)-H(2)	1.10(3)
Co-C(1)	2.088(4)	B(1)-H(3)	1.27(4)
Co-C(2)	2.098(4)	B(2)-B(3)	1.798(10)
Co-C(3)	2.110(4)	B(2)-H(4)	1.10(3)
Co-C(4)	2.085(3)	B(2)-H(5)	1.25(4)
Co-C(5)	2.063(4)	B(3)-H(6)	1.11(3)
Co-C(11)	1.736(5)	B(3)-H(7)	1.11(3)
C(11)-O	1.151(5)		
C(11)-Co-B(2)	108.1(3)	B(1)-B(2)-H(3)	43(2)
C(11)-Co-B(3)	80.5(3)	Co-B(2)-H(3)	108(2)
B(2)-Co-B(3)	51.9(3)	B(3)-B(2)-H(4)	120(3)
C(11)-Co-B(1)	82.0(2)	B(1)-B(2)-H(4)	127(3)
B(2)-Co-B(1)	53.5(3)	Co-B(2)-H(4)	116(3)
B(3)-Co-B(1)	90.5(3)	H(3)-B(2)-H(4)	115(4)
O-C(11)-Co	176.3(5)	B(3)-B(2)-H(5)	44(2)
B(2)-B(1)-Co	60.9(3)	B(1)-B(2)-H(5)	130(3)
B(2)-B(1)-H(1)	130(2)	Co-B(2)-H(5)	111(2)
Co-B(1)-H(1)	129(2)	H(3)-B(2)-H(5)	106(4)
B(2)-B(1)-H(2)	116(3)	H(4)-B(2)-H(5)	101(4)
Co-B(1)-H(2)	115(3)	B(2)-B(3)-Co	61.7(3)
H(1)-B(1)-H(2)	102(3)	B(2)-B(3)-H(5)	44(2)
B(2)-B(1)-H(3)	42(2)	Co-B(3)-H(5)	106(2)
Co-B(1)-H(3)	102(2)	B(2)-B(3)-H(6)	122(3)
H(1)-B(1)-H(3)	111(3)	Co-B(3)-H(6)	115(3)
H(2)-B(1)-H(3)	92(4)	H(5)-B(3)-H(6)	103(4)
B(3)-B(2)-B(1)	109.3(5)	B(2)-B(3)-H(7)	123(3)
B(3)-B(2)-Co	66.4(3)	Co-B(3)-H(7)	121(3)
B(1)-B(2)-Co	65.6(3)	H(5)-B(3)-H(7)	101(4)
B(3)-B(2)-H(3)	121(3)	H(6)-B(3)-H(7)	108(4)

arachno-Cp*(CO)CoB₃H₇, 3. The molecular structure of **3** is shown in Figure 2, and selected distances and angles are given in Table 4. Here too, all of the parameters fall within the ranges of existing structural data on boranes³⁷ and metallaboranes.³⁸ As [B₃H₇]²⁻ is isoelectronic with [C₃H₅]⁻, compounds containing this species are often called borallyl complexes. Thus, just as boranes have isoelectronic carbocation partners, so too, **3** is isoelectronic with [CpCo(CO)(C₃H₅)⁺.⁴³ There are known borallyl complexes of Ir,^{25,26} Pd,^{27,28} and Pt.²⁹⁻³¹ Compound **3** is the first example which contains

Table 5. Comparison of the Structural Parameters of $[(\text{CH}_3)_2\text{NPF}_2\text{BH}]_3\text{B}_3\text{H}_7$, *arachno*-($\eta^5\text{-C}_5\text{Me}_5$)(CO)CoB₃H₇, **3**, and Known Borallyl Complexes


	M–B1 (Å)	M–B2 (Å)	M–B3 (Å)	B1–B2 (Å)	B2–B3 (Å)	B1–B2–B3 (deg)	B1–M–B2 (deg)	B2–M–B3 (deg)	B1–M–B3 (deg)
$\{(\text{CH}_3)_2\text{NPF}_2\text{BH}\}_3\text{B}_3\text{H}_7^a$				1.759(13)	1.753(14)	114.1(7)			
$[\text{Cp}^*\text{Co}(\text{CO})\text{B}_3\text{H}_7]^b$	2.098(6)	2.014(6)	2.096(6)	1.853(11)	1.798(10)	109.3(5)	53.5(3)	51.9(3)	90.5(3)
$[(\text{Ph}_3)_2\text{IrH}(\text{CO})\text{B}_3\text{H}_7]^c$	2.229(8)	2.197(8)	2.303(8)	1.829(11)	1.837(11)	112.9(6)	48.1(3)	47.9(3)	83.2(3)
$[(\text{dppf})\text{PdB}_3\text{H}_7]^d$	2.190(3)	2.154(3)	2.182(3)	1.792(5)	1.787(5)	112.0(3)	48.7(1)	48.7(1)	85.5(1)
$[(\text{dppe})\text{PdB}_3\text{H}_7]^e$	2.173(12)	2.119(12)	2.160(13)	1.846(16)	1.791(17)	114.3(8)	50.9(4)	49.5(5)	89.7(5)
$[(\text{dppb})\text{PdB}_3\text{H}_7]^e$	2.193(10)	2.135(15)	2.192(14)	1.772(26)	1.729(21)	119.3(10)	48.3(7)	47.1(6)	87.1(7)
$[(\text{PPh}_3)_2\text{PtB}_3\text{H}_7]^f$	2.188(17)	2.149(16)	2.223(20)	1.750(30)	1.890(30)	113.2(12)	48.2(6)	50.2(7)	86.7(7)

^a Reference 45. ^b This work. ^c Reference 26. ^d Reference 28. ^e Reference 27. ^f Reference 29.

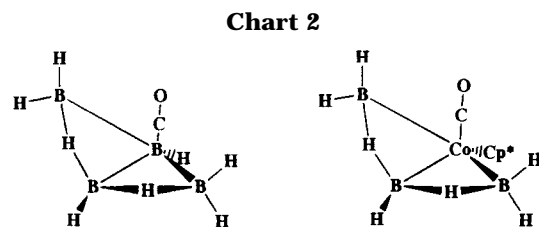
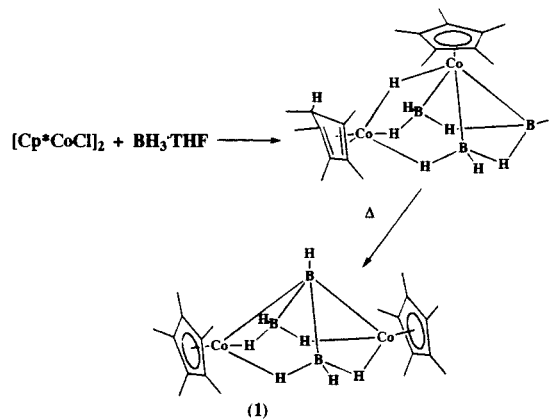
**Figure 2.** Molecular structure of *arachno*-Cp*(CO)CoB₃H₇, **3**, with thermal ellipsoids at 40% probability.

a first-row transition metal, and a comparison of selected structural parameters with those of known compounds is given in Table 5. Relative to the differences in the covalent radii, the Co–B distances range from 0.02 to 0.10 Å shorter than those of the heavier metals. The B(1)–B(2)–B(3) angle in **3** is at the low end of the range of the other compounds, and consistently, the B(1)–M–B(3) angle is at the high end of the range of the other compounds.

There are striking differences between the ¹¹B NMR shifts for these compounds, but these are due to the different metals (and ligands) rather than structural or bonding effects. That is, the difference in the shift between B(2) and B(1,3) is ~16 for Pt,²⁹ 11 for Pd,²⁷ 18 for Ir,²⁵ and 7 for Co, suggesting a decrease of 5–6 ppm in going from third-row to second-row to first-row transition metals. This is consistent with past experience. Further, both boron resonances of **3** lie downfield of those of the Ir compound, which is again consistent with observations of other related metallaboranes.

Usually borallyl complexes have been related to seven sep *arachno*-B₄H₁₀ in which a BH₃ unit has been replaced by the metal fragment. The structural parameters of the B₃H₇ fragment match those of the same fragment in B₄H₁₀ well and differ considerably from those in *nido*-**2** and its analogues.⁴⁴ The same analysis

(43) Elschenbroich, C.; Salzer, A. *Organometallics*; VCH: New York, 1989.

**Chart 2****(1)**

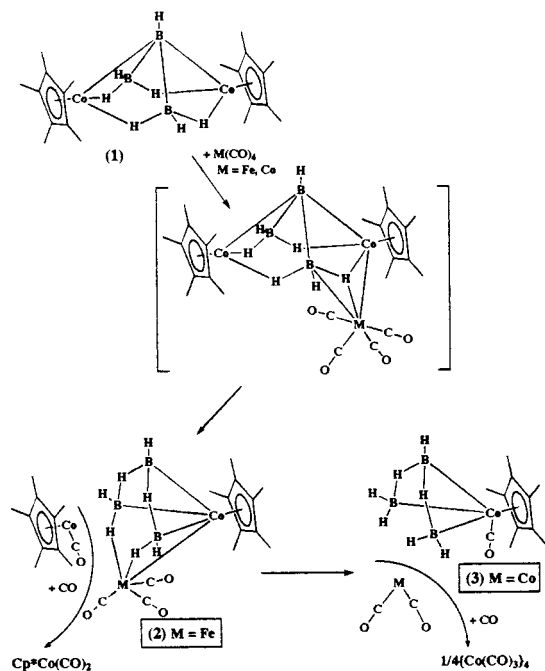
holds for **3**, but a more pleasing comparison is with the structure of B₄H₈CO (based on the structure of B₄H₈PF₂N(CH₃)₂)⁴⁵ as shown in Chart 2 (structural parameters in Table 5). If a single BH is replaced by Cp*Co, then the two structures are completely analogous in terms of the relative orientations of the H's as well as the CO ligand.

Reaction Pathway. The reaction of $[\text{Cp}^*\text{CoCl}]_2$ with $\text{BH}_3 \cdot \text{THF}$ initially leads to *nido*-1,2-(Cp*Co)(μ-H){(η^4 -C₅Me₅H)Co}B₃H₇ (Chart 3), which was isolated in good yield and fully characterized.¹⁶ The investigation of the reactions of this compound with both main-group species as well as metal-fragment sources gave disappointing results. Only in the case of Fe₂(CO)₉ were there any signs of success. Here, Cp*Co(CO)₂ was found accompanied by very small quantities of a compound identified spectroscopically as **2**. As **2** probably came from **1**

(44) Housecroft, C. E.; Fehlner, T. P. *Inorg. Chem.* **1982**, *21*, 1739.

(45) LaPrade, M. D.; Nordman, C. E. *Inorg. Chem.* **1969**, *8*, 1669.

Chart 4



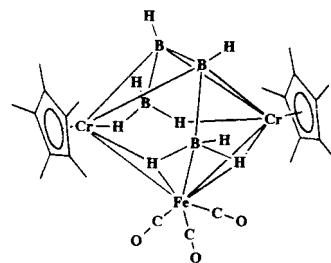
formed during reaction, this work implies that *nido*-1,2- $(\text{Cp}^*\text{Co})(\mu\text{-H})\{\eta^4\text{-C}_5\text{Me}_5\text{H}\text{Co}\}\text{B}_3\text{H}_7$ does not react directly with the reagents examined.

The non-boron-containing coproducts provide evidence of the reaction pathway. In both reactions, copious quantities of $\text{Cp}^*\text{Co}(\text{CO})_2$ are observed, and in the case of $\text{Co}_2(\text{CO})_8$, $\text{Co}_4(\text{CO})_{12}$ is observed as well. As CO is known to cleave cluster frameworks and is present in the reactions of metal carbonyls, the control reaction of **1** with CO was carried out. Stirring a solution of **1** for 44 h at 23 °C in 1 atm of CO resulted in the formation of traces of $\text{Cp}^*\text{Co}(\text{CO})_2$, and **1** was recovered. Importantly, no sign of **3** was observed, suggesting that $\text{Co}_2(\text{CO})_8$ plays a more important role than simply acting as a source of CO.

These observations lead us to postulate the reaction pathway shown in Chart 4. Formation of $M(\text{CO})_4$, $M = \text{Fe}$ and Co , from $\text{Fe}_2(\text{CO})_9$ and $\text{Co}_2(\text{CO})_8$, respectively, is followed by coordination of the M center to a B–H–Co edge to yield the unobserved intermediate depicted in brackets. Support for this postulate comes from the reaction of B_6H_{10} with $\text{Fe}_2(\text{CO})_9$ to form $\text{B}_6\text{H}_{10}\text{Fe}(\text{CO})_4$ in which the Fe lies below the cage and bridges the B–B edge of hexaborane.⁴⁶ Although there is no triply bridging hydride in this compound, the reaction of $(\text{Cp}^*\text{Cr})_2\text{B}_4\text{H}_8$ with $\text{Fe}_2(\text{CO})_9$ to form $(\text{Cp}^*\text{Cr})_2\text{B}_4\text{H}_8\{\text{Fe}(\text{CO})_3\}$ (Chart 5) provides additional support.⁴⁷ Here, the $\text{Fe}(\text{CO})_3$ fragment interacts with two Cr–H–B bridges yielding two triply bridging hydrogens. Thus, the chromium compound could very well arise by loss of CO from an $\text{Fe}(\text{CO})_4$ adduct of $(\text{Cp}^*\text{Cr})_2\text{B}_4\text{H}_8$, i.e., an intermediate analogous to that shown in Chart 4.

The next step in both reactions of **1** is the transfer of one CO to one Cp^*Co fragment followed by release of $\text{Cp}^*\text{Co}(\text{CO})$, which presumably rapidly scavenges another CO to form the observed $\text{Cp}^*\text{Co}(\text{CO})_2$ product. For iron, the reaction stops here, having generated the

Chart 5



observed product with the Fe atom in a basal position. Heating **2** for 14 h at 85 °C followed by 2 h at 100 °C led to neither rearrangement nor decomposition. Recently, we have found that skeletal rearrangement in a dirhodapentaborane proceeds to completion under considerably milder conditions.¹⁷ Thus, **2** is the most stable isomer, and the isomer observed is not mechanistically meaningful.

In the case of the reaction of **1** with $\text{Co}_2(\text{CO})_8$, further transformation takes place as shown in Chart 4. Elimination of the cobalt carbonyl fragment, which scavenges a CO to form $\text{Co}_4(\text{CO})_{12}$, leads to **3**. Although in this case a Co fragment is lost, the reaction of $(\text{Cp}^*\text{Cr})_2\text{B}_4\text{H}_8$ with $\text{Co}_2(\text{CO})_8$ gives $(\text{Cp}^*\text{Cr})_2\text{B}_4\text{H}_7\{\text{Co}(\text{CO})_3\}$ in good yield.²² The initial adduct in both cases would have an odd electron, but in one case, a cobalt carbonyl radical is lost to yield **3** and $1/4\text{Co}_4(\text{CO})_{12}$, and in the other case, a hydrogen atom is lost to yield $(\text{Cp}^*\text{Cr})_2\text{B}_4\text{H}_7\{\text{Co}(\text{CO})_3\}$ and $1/2\text{H}_2$. The origin of these differing behaviors is not known. Only when more information on reactivity is compiled will answers to these subtle, but important, mechanistic questions be forthcoming.

Reactions of metal fragments with organometallic clusters are well-studied if not well-understood.²³ Both fragment-addition reactions as well as fragment-substitution reactions have been documented. Many of the observations concern tetrahedral M_3E clusters,^{48,49} and in at least one instance involving $\text{Co}_2(\text{CO})_8$, the presence of a radical pathway is strongly implicated.⁵⁰ Addition as well as substitution reactions have been observed in ferraborane chemistry.^{24,51} On the other hand, although cluster degradation by Lewis bases is well-established,⁵² the effective degradation by a metal fragment, as seen in the formation of **3**, is not. Undoubtedly it takes place but may be hidden in many cases by the complexity of the systems.

Acknowledgment. The generous support of the National Science Foundation is gratefully acknowledged. We also thank Dr. Y. Nishihara and Ms. A. K. McCasland for aid with the preliminary experiments.

Supporting Information Available: Tables of crystallographic parameters, atomic coordinates, equivalent isotropic temperature factors, anisotropic temperature factors, bond distances, and bond angles for **2** and **3** (31 pages). Ordering information is given on any current masthead page.

OM980010X

(48) Vahrenkamp, H.; Wucherer, E. *J. Angew. Chem., Int. Ed. Engl.* **1981**, *20*, 680.

(49) Vahrenkamp, H. *J. Organomet. Chem.* **1989**, *370*, 65.

(50) Horwitz, C. P.; Holt, E. M.; Shriver, D. F. *Organometallics* **1985**, *4*, 1117.

(51) Bandyopadhyay, A.; Shang, M.; Jun, C.-S.; Fehner, T. P. *Inorg. Chem.* **1994**, *33*, 3677.

(52) Lewis, J.; Johnson, B. F. G. *Pure Appl. Chem.* **1982**, *54*, 97.

(46) Davison, A.; Traficante, D. D.; Wreford, S. S. *Chem. Commun.* **1972**, 1155.

(47) Hashimoto, H.; Shang, M.; Fehner, T. P. *J. Am. Chem. Soc.* **1996**, *118*, 8164.